

Low-energy magnetic dipole strength in cadmium isotopesR. Schwengner *Helmholtz-Zentrum Dresden-Rossendorf, 01328 Dresden, Germany*

(Received 15 October 2021; accepted 20 December 2021; published 3 January 2022)

Magnetic-dipole strength functions have been deduced from averages of large numbers of $M1$ transition strengths calculated within the shell model for the nuclides ^{105}Cd , ^{106}Cd , ^{111}Cd , and ^{112}Cd . Enhancements of the $M1$ strengths toward low transition energy have been found for all nuclides considered. These properties are compared with those of experimental photon strength functions obtained from ^3He -induced reactions, which seem to indicate a disappearance of the low-energy enhancement in the heavier isotopes.

DOI: [10.1103/PhysRevC.105.014303](https://doi.org/10.1103/PhysRevC.105.014303)**I. INTRODUCTION**

The investigation of properties of γ -ray strength functions has been the subject of numerous experimental and theoretical efforts in the past years. By describing average transition strengths in a certain range of high excitation energy and high level density, γ -ray strength functions are a main input to calculations of reaction rates within statistical reaction models. These calculations are used, for example, to obtain information about neutron-capture cross sections of unstable nuclides. The strength function at high energy is dominated by the isovector giant dipole resonance (GDR) and has been approached by Lorentz functions. A number of new phenomena has been found on top of the low-energy tail of the GDR, such as the pygmy dipole resonance (PDR) between about 6 and 10 MeV also consisting of electric-dipole ($E1$) excitations [1–3], the scissors mode in deformed nuclides around 3 MeV based on magnetic-dipole ($M1$) excitations [4], and the low-energy enhancement or so-called upbend, an increase of dipole strength with decreasing γ -ray energy below about 2 MeV. It was shown that the PDR affects neutron-capture rates determining the path of the astrophysical s -process of the nucleosynthesis [5,6], while the pronounced enhancement of the dipole strength at low γ -ray energy may have a potentially large impact on neutron-capture reaction rates of very neutron-rich nuclides occurring in the r -process [7].

The low-energy enhancement has been observed in a number of nuclides in various mass regions, mainly using light-ion-induced reactions in connection with the so-called Oslo method to extract level densities and γ -ray strength functions. These studies started with $^{56,57}\text{Fe}$ [8] and continued to heavier nuclides, for example, Ge isotopes [9], Y isotopes [10], Mo isotopes [11], Cd isotopes [12], and Sm isotopes [13,14]. The Oslo method was also applied in connection with β decay of ^{76}Ga [15]. A dominant dipole character of the low-energy strength was demonstrated in Ref. [16] and

an indication for an $M1$ character was discussed for the case of ^{60}Ni [17]. An exceptional case is represented by the Cd isotopes. The light isotope ^{105}Cd shows the upbend below about 1.5 MeV, whereas the strength functions of the neighbor ^{106}Cd and of the heavier isotopes ^{111}Cd and ^{112}Cd do not show an upbend [12]. Possible reasons for this behavior, speculated in Ref. [12], may be the uncovering of a mass region exhibiting the onset of the low-energy enhancement.

To understand the mechanism producing the enhanced strength at low energy, various model calculations have been performed. Shell-model calculations revealed that a large number of $M1$ transitions between excited states produces an exponential increase of the γ -ray strength function that peaks at $E_\gamma \approx 0$ and describes the low-energy enhancement of dipole strength observed in Mo isotopes around the neutron shell closure at $N = 50$ [18]. Large $B(M1)$ transition strengths appear for transitions linking states with configurations dominated by both protons and neutrons in high- j orbitals, the spins of which recouple. The low-energy enhancement of $M1$ strength was confirmed in shell-model calculations for $^{56,57}\text{Fe}$ [19] and ^{44}Sc [20]. In the latter work, also the $E1$ strength function was calculated, which does not show an upbend comparable to that of the $M1$ strength. A correlation between the low-energy $M1$ strength and the scissors mode was found in shell-model calculations for the series of isotopes from ^{60}Fe to ^{68}Fe [21]. The low-energy $M1$ strength decreases and the scissors strength develops when going into the open shell. The simultaneous appearance of the two modes is in accordance with experimental findings in Sm isotopes [13,14]. Later on, $M1$ strength functions have been calculated for isotopic series in several mass regions from $Z = 8$ to 32 [22,23] and $Z = 52$ to 58 [24]. These shell-model studies confirmed that the low-energy enhancement of $M1$ strength appears in almost all nuclides studied and is strongest in nuclides near shell closures. The only cases without a low-energy enhancement are the $N = Z$ nuclides ^{48}Cr [25] and ^{108}Xe [24].

With respect to those results, the trends of the strength functions observed in the Cd isotopes remain an open issue for the understanding of the occurrence of the low-energy enhancement as a general feature. As an approach to

*r.schwengner@hzdr.de

this problem, this work presents predictions of shell-model calculations for the $M1$ strength functions of the Cd isotopes and confronts these with the experimental findings.

II. SHELL-MODEL CALCULATIONS

The shell-model calculations for the cadmium isotopes were carried out in the $jj45pn$ model space with the $jj45pna$ Hamiltonian using the code `NUSHELLX@MSU` [26]. The method used to obtain the $jj45pna$ two-body matrix elements is described in Ref. [27]. For the application below ^{132}Sn , the single-particle energies were adjusted to reproduce the experimental spectrum of ^{131}Sn and ^{131}In . The energies for the $2p_{3/2}$ and $1f_{5/2}$ proton hole states were taken from energy-density-functional calculations [28]. The model space included the proton orbitals ($1f_{5/2}, 2p_{3/2}, 2p_{1/2}, 1g_{9/2}$) and the neutron orbitals ($1g_{7/2}, 2d_{5/2}, 2d_{3/2}, 2s_{1/2}, 1h_{11/2}$). To make the calculations feasible, the configuration spaces were truncated. Two protons were allowed to be excited from the (fp) orbitals to the $1g_{9/2}$ orbital. In ^{105}Cd and ^{106}Cd , at least three neutrons occupied the $1g_{7/2}$ and at least two occupied the $2d_{5/2}$ orbital. One neutron could be lifted to each of the ($2d_{3/2}, 2s_{1/2}$) orbitals and up to two to the $1h_{11/2}$ orbital. In ^{111}Cd and ^{112}Cd , at least six neutrons occupied the $1g_{7/2}$ and at least four occupied the $2d_{5/2}$ orbital. Up to two neutrons could be lifted to each of the ($2d_{3/2}, 2s_{1/2}, 1h_{11/2}$) orbitals. Reduced electric-quadrupole transition strengths $B(E2)$ were calculated by applying effective charges of $e_\pi = 1.6e$ and $e_\nu = 1.0e$, as used in recent calculations of $B(E2)$ values between low-lying states in ^{106}Cd [29].

The 2_1^+ state in ^{106}Cd was calculated at $E(2_1^+)_{\text{calc}} = 0.480$ MeV, compared with an experimental value of $E(2_1^+)_{\text{expt}} = 0.633$ MeV. The calculated strength of the ground-state transition, $B(E2, 2_1^+ \rightarrow 0_1^+)_{\text{calc}} = 718 e^2 \text{fm}^4$, is compatible with the experimental value of $B(E2, 2_1^+ \rightarrow 0_1^+)_{\text{expt}} = 769(9) e^2 \text{fm}^4$. The corresponding values for ^{112}Cd are $E(2_1^+)_{\text{calc}} = 0.468$ MeV, $E(2_1^+)_{\text{expt}} = 0.618$ MeV, $B(E2, 2_1^+ \rightarrow 0_1^+)_{\text{calc}} = 905 e^2 \text{fm}^4$, and $B(E2, 2_1^+ \rightarrow 0_1^+)_{\text{expt}} = 972(6) e^2 \text{fm}^4$. In the heavier isotopes, more than two neutrons may be lifted to the $1h_{11/2}$ orbital. To enable this in the calculations, stronger limitations have to be applied to the other neutron orbitals. With at least five neutrons in the $2d_{5/2}$ orbital, at most one in each of the ($2d_{3/2}, 2s_{1/2}$) orbitals, and still up to two in the $1h_{11/2}$ orbital, one obtains a reduction of the $B(E2, 2_1^+ \rightarrow 0_1^+)_{\text{calc}}$ value to $692 e^2 \text{fm}^4$ in ^{112}Cd . At the same time, the low-energy $M1$ upbend gets steeper and the peak near $E_\gamma = 0$ increases by a factor of about two. Such an increase is a typical effect appearing when making the configuration space small. Besides, stronger fluctuations appear in the region of the scissors mode that are caused by strong transitions concentrated in particular energy bins and weak transitions in other bins, and the spectrum continues to higher energy including dominant transitions beyond 4 MeV. Allowing up to three neutrons in the $1h_{11/2}$ orbital along with the other limitations just mentioned, one obtains similar values, $B(E2, 2_1^+ \rightarrow 0_1^+)_{\text{calc}} = 634 e^2 \text{fm}^4$ and a slightly higher peak of the upbend near $E_\gamma = 0$, while the mean neutron numbers in the $1h_{11/2}$ orbital do not considerably

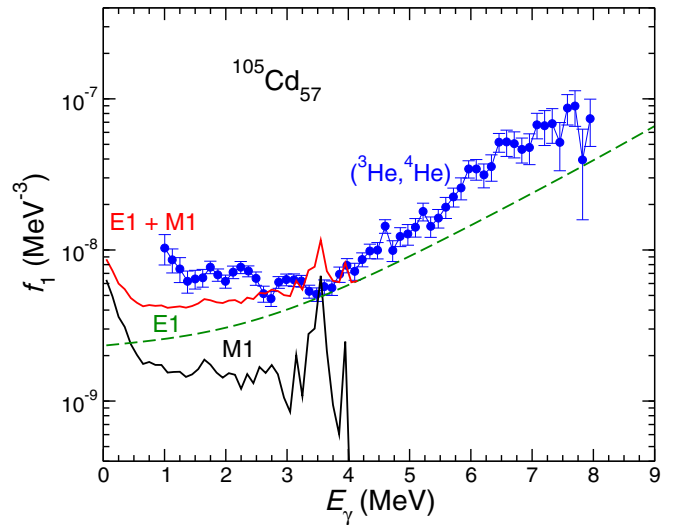


FIG. 1. $M1$ strength function for ^{105}Cd deduced from the present shell-model calculations (black solid line), $E1$ strength function based on the GLO model (green dashed line), the sum of the $M1$ and $E1$ strength functions (red solid line), and experimental data (blue circles) taken from Ref. [12].

exceed the number of two in most states. The calculations described in the following refer to the limitations given first in this section.

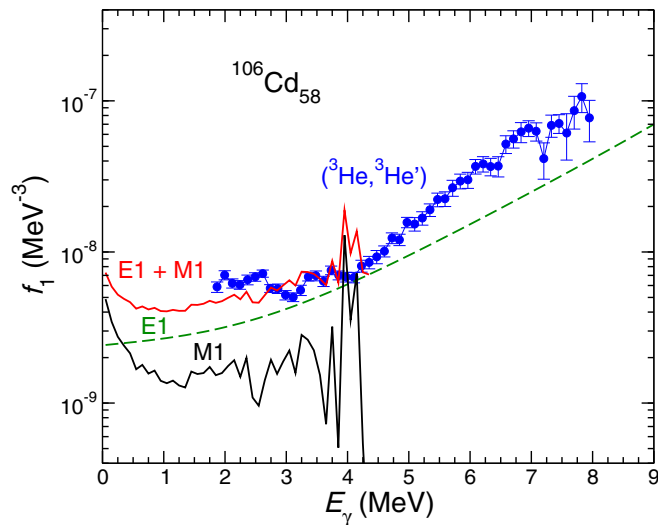
The calculations were performed for the lowest 40 states of each spin from 0 to 10 and each parity. Reduced magnetic-dipole transition strengths $B(M1)$ were calculated by applying effective g factors of $g_s^{\text{eff}} = 0.7g_s^{\text{free}}$ for all transitions from initial to final states with energies $E_i > E_f$ and spins $J_i = J_f, J_f \pm 1$. This resulted in about 24 000 $M1$ transitions. $M1$ strength functions were deduced according to

$$f_{M1}(E_\gamma, E_i, J_i, \pi) = 16\pi/9(\hbar c)^{-3} \bar{B}(M1, E_i \rightarrow E_f, J_i, \pi) \times \rho(E_i, J_i, \pi), \quad (1)$$

with $E_\gamma = E_i - E_f$, where the $\bar{B}(M1, E_i \rightarrow E_f, J_i, \pi)$ are averages in the (E_i, E_f) bins considered for given J_i, π ; and $\rho(E_i, J_i, \pi)$ are level densities derived from the present calculations. The strength functions $f_{M1}(E_\gamma)$ were obtained by averaging step-by-step over E_i, J_i , and π .

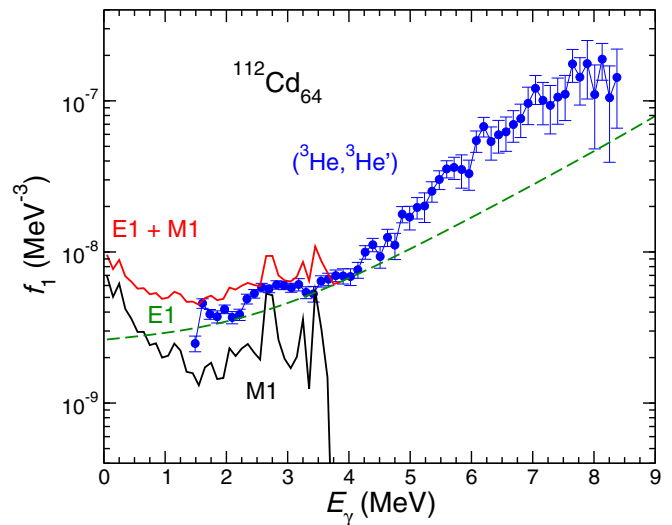
III. RESULTS

For a comparison with the experimental dipole strength functions f_1 determined in Ref. [12], an $E1$ part had to be added to the present calculated $M1$ strength functions. Because the data in Ref. [12] were compared with the generalized Lorentzian (GLO) model [30,31], this was also used here with identical parameters for the $E1$ strength. The $M1$ and $E1$ strength functions as well as their sums are graphed for the considered isotopes in Figs. 1–4 together with the experimental data from Ref. [12]. Note that the calculated $M1$ strength functions have uncertainties arising from model-space limitations and the GLO model for the $E1$ strength function is an extrapolation from the GDR toward low energy including uncertainties of the specific parameters such as the

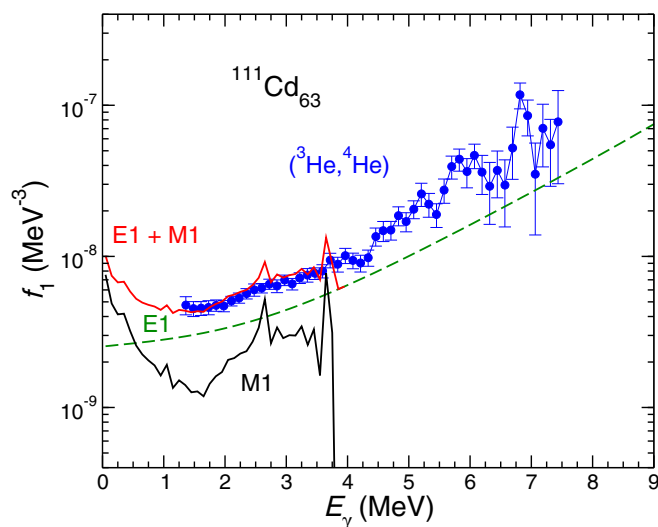
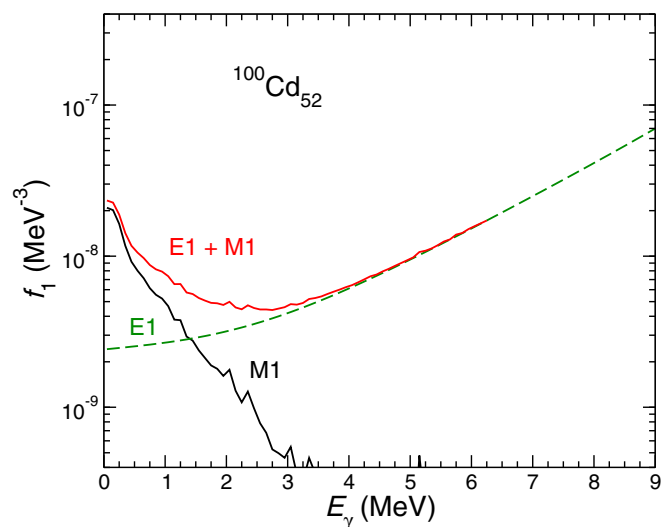

 FIG. 2. Same as Fig. 1, but for ^{106}Cd .

nuclear temperature. Therefore, the comparison of calculated with experimental data serves to show general trends of the strength functions rather than to give a precise quantitative description of the experimental data.

The $M1$ strength functions in all four isotopes show an enhancement toward $E_\gamma = 0$ below about 1 MeV. Toward high energy, the upbend is followed by a saddle and a bump between about 2 and 4 MeV. This bump corresponds to the one seen in open-shell Fe [21] and Sm isotopes [13,14] and is considered as a scissor-like resonance. Prominent peaks in the high-energy part of the $M1$ strength function arise from strong transitions from the highest calculated levels to the ground or first-excited states. These dominate the average strength because of the small number of transitions in the highest-energy bins and hence overestimate the $M1$ strength function at the upper end of the calculated spectrum. All total ($E1 + M1$) strength functions f_1 also exhibit the low-energy enhancement. In ^{105}Cd , the calculated f_1 lies below the ex-


 FIG. 4. Same as Fig. 1, but for ^{112}Cd .

perimental one. This is similar to the situation in previous calculations, for example, in $^{94-96}\text{Mo}$ [18] and $^{56,57}\text{Fe}$ [19], and may indicate that the calculated $M1$ strength does not fully account for the experimental one at nucleon numbers not far from closed shells. Besides, the enhancement starts below about 0.7 MeV, whereas the experimental one reaches to about 1.5 MeV. In ^{106}Cd , calculated and experimental f_1 behave similarly between about 2 and 4 MeV. There are no experimental data below about 2 MeV and hence no information about a possible upbend. In the heavier isotope ^{111}Cd , a good agreement between calculated and experimental f_1 is seen between about 1.5 and 4 MeV. Also in this isotope the upbend in the calculated f_1 starts where the experimental data stop. In ^{112}Cd , a beginning upbend may be indicated by the three experimental values below 2 MeV, but the value at the lowest energy is considerably smaller, in contrast with the calculated f_1 that starts to increase at about this energy.


 FIG. 3. Same as Fig. 1, but for ^{111}Cd .

 FIG. 5. Same as Fig. 1, but for ^{100}Cd . There are no experimental data available for this nuclide.

To reveal the development of the low-energy $M1$ strength with nucleon numbers approaching shell closures, the $M1$ strength function was also calculated for the $N = 52$ isotope ^{100}Cd . The results are shown in Fig. 5. The f_{M1} reaches about twice the magnitude at $E_\gamma \approx 0$ compared with the heavier isotopes. It shows a steady decrease toward high energies, while the bump between 2 and 4 MeV seen in the heavier isotopes disappears. The increase of the low-energy strength and the disappearance of the scissors-like resonance when approaching shell closures is consistent with the properties found for the series of Fe isotopes [21].

IV. CONCLUSIONS

$M1$ strength functions deduced from shell-model calculations for the isotopes ^{100}Cd , ^{105}Cd , ^{106}Cd , ^{111}Cd , and ^{112}Cd do not confirm a disappearance of the low-energy enhancement of dipole strength in the heavier isotopes, which was suspected on the basis of experimental data. The low-energy enhancement of $M1$ strength is present in all isotopes. However, it gets

weaker when going into the open neutron shell, while a bump develops in the region of the scissors resonance. This behavior resembles the properties of $M1$ strength found in other mass regions. Except for ^{105}Cd , the calculated low-energy upbend is below the lowest energies, for which experimental data are available. Therefore, a definite conclusion about the appearance of the upbend is not possible on the basis of the existing data. A more comprehensive study of the behavior of the strength functions at very low energy in ^{111}Cd and ^{112}Cd on the basis of new high-resolution experiments may clarify the situation.

ACKNOWLEDGMENTS

I thank K. Sieja for stimulating discussions and B.A. Brown for his support in using the code NUSHELLX@MSU. The allocation of computing time through the Centers for High-Performance Computing of Technische Universität Dresden and of Helmholtz-Zentrum Dresden-Rossendorf is gratefully acknowledged.

-
- [1] G. A. Bartholomew, E. D. Earle, A. J. Ferguson, J. W. Knowles, and M. A. Lone, in *Advances in Nuclear Physics*, edited by M. Baranger and E. Vogt (Springer, Boston, 1973), Vol. 7, pp. 229–324.
- [2] D. Savran, T. Aumann, and A. Zilges, *Prog. Part. Nucl. Phys.* **70**, 210 (2013).
- [3] A. Bracco, E. G. Lanza, and A. Tamii, *Prog. Part. Nucl. Phys.* **106**, 360 (2019).
- [4] K. Heyde, P. von Neumann-Cosel, and A. Richter, *Rev. Mod. Phys.* **82**, 2365 (2010).
- [5] M. Beard, S. Frauendorf, B. Kämpfer, R. Schwengner, and M. Wiescher, *Phys. Rev. C* **85**, 065808 (2012).
- [6] N. Tsoneva, S. Goriely, H. Lenske, and R. Schwengner, *Phys. Rev. C* **91**, 044318 (2015).
- [7] A. C. Larsen and S. Goriely, *Phys. Rev. C* **82**, 014318 (2010).
- [8] A. Voinov, E. Algin, U. Agvaanlusan, T. Belgia, R. Chankova, M. Guttormsen, G. E. Mitchell, J. Rekstad, A. Schiller, and S. Siem, *Phys. Rev. Lett.* **93**, 142504 (2004).
- [9] T. Renstrøm, H.-T. Nyhus, H. Utsunomiya, R. Schwengner, S. Goriely, A. C. Larsen, D. M. Filipescu, I. Gheorghe, L. A. Bernstein, D. L. Bleuel, T. Glodariu, A. Gørgen, M. Guttormsen, T. W. Hagen, B. V. Kheswa, Y.-W. Lui, D. Negi, I. E. Ruud, T. Shima, S. Siem *et al.*, *Phys. Rev. C* **93**, 064302 (2016).
- [10] A. C. Larsen, M. Guttormsen, R. Schwengner, D. L. Bleuel, S. Goriely, S. Harissopulos, F. L. Bello Garrote, Y. Byun, T. K. Eriksen, F. Giacoppo, A. Gørgen, T. W. Hagen, M. Klintefjord, T. Renstrøm, S. J. Rose, E. Sahin, S. Siem, T. G. Tornyi, G. M. Tveten, A. V. Voinov, and M. Wiedeking, *Phys. Rev. C* **93**, 045810 (2016).
- [11] M. Guttormsen, R. Chankova, U. Agvaanlusan, E. Algin, L. A. Bernstein, F. Ingebretsen, T. Lönnroth, S. Messelt, G. E. Mitchell, J. Rekstad, A. Schiller, S. Siem, A. C. Sunde, A. Voinov, and S. Ødegård, *Phys. Rev. C* **71**, 044307 (2005).
- [12] A. C. Larsen, I. E. Ruud, A. Bürger, S. Goriely, M. Guttormsen, A. Gørgen, T. W. Hagen, S. Harissopulos, H. T. Nyhus, T. Renstrøm, A. Schiller, S. Siem, G. M. Tveten, A. Voinov, and M. Wiedeking, *Phys. Rev. C* **87**, 014319 (2013).
- [13] A. Simon, M. Guttormsen, A. C. Larsen, C. W. Beausang, P. Humby, J. T. Burke, R. J. Casperson, R. O. Hughes, T. J. Ross, J. M. Allmond, R. Chyzh, M. Dag, J. Koglin, E. McCleskey, M. McCleskey, S. Ota, and A. Saastamoinen, *Phys. Rev. C* **93**, 034303 (2016).
- [14] F. Naqvi, A. Simon, M. Guttormsen, R. Schwengner, S. Frauendorf, C. S. Reingold, J. T. Burke, N. Cooper, R. O. Hughes, S. Ota, and A. Saastamoinen, *Phys. Rev. C* **99**, 054331 (2019).
- [15] A. Spyrou, S. N. Liddick, A. C. Larsen, M. Guttormsen, K. Cooper, A. C. Dombos, D. J. Morrissey, F. Naqvi, G. Perdikakis, S. J. Quinn, T. Renstrøm, J. A. Rodriguez, A. Simon, C. S. Sumithrarachchi, and R. G. T. Zegers, *Phys. Rev. Lett.* **113**, 232502 (2014).
- [16] A. C. Larsen, N. Blasi, A. Bracco, F. Camera, T. K. Eriksen, A. Gørgen, M. Guttormsen, T. W. Hagen, S. Leoni, B. Million, H. T. Nyhus, T. Renstrøm, S. J. Rose, I. E. Ruud, S. Siem, T. Tornyi, G. M. Tveten, A. V. Voinov, and M. Wiedeking, *Phys. Rev. Lett.* **111**, 242504 (2013).
- [17] A. Voinov, S. M. Grimes, C. R. Brune, M. Guttormsen, A. C. Larsen, T. N. Massey, A. Schiller, and S. Siem, *Phys. Rev. C* **81**, 024319 (2010).
- [18] R. Schwengner, S. Frauendorf, and A. C. Larsen, *Phys. Rev. Lett.* **111**, 232504 (2013).
- [19] B. A. Brown and A. C. Larsen, *Phys. Rev. Lett.* **113**, 252502 (2014).
- [20] K. Sieja, *Phys. Rev. Lett.* **119**, 052502 (2017).
- [21] R. Schwengner, S. Frauendorf, and B. A. Brown, *Phys. Rev. Lett.* **118**, 092502 (2017).
- [22] S. Karampagia, B. A. Brown, and V. Zelevinsky, *Phys. Rev. C* **95**, 024322 (2017).
- [23] J. E. Midtbø, A. C. Larsen, T. Renstrøm, F. L. Bello Garrote, and E. Lima, *Phys. Rev. C* **98**, 064321 (2018).
- [24] K. Sieja, *Phys. Rev. C* **98**, 064312 (2018).
- [25] K. Sieja, *EPJ Web Conf.* **146**, 05004 (2017).

- [26] B. A. Brown and W. D. M. Rae, [Nucl. Data Sheets](#) **120**, 115 (2014).
- [27] J. Shergur, B. A. Brown, V. Fedoseyev, U. Köster, K.-L. Kratz, D. Seweryniak, W. B. Walters, A. Wöhr, D. Fedorov, M. Hannawald, M. Hjorth-Jensen, V. Mishin, B. Pfeiffer, J. J. Ressler, H. O. U. Fynbo, P. Hoff, H. Mach, T. Nilsson, K. Wilhelmsen-Rolander, H. Simon *et al.*, and the ISOLDE Collaboration, [Phys. Rev. C](#) **65**, 034313 (2002).
- [28] B. A. Brown (private communication).
- [29] D. Rhodes, B. A. Brown, J. Henderson, A. Gade, J. Ash, P. C. Bender, R. Elder, B. Elman, M. Grindler, M. Hjorth-Jensen, H. Iwasaki, B. Longfellow, T. Mijatović, M. Spieker, D. Weisshaar, and C. Y. Wu, [Phys. Rev. C](#) **103**, L051301 (2021).
- [30] J. Kopecky and R. E. Chrien, [Nucl. Phys. A](#) **468**, 285 (1987).
- [31] J. Kopecky and M. Uhl, [Phys. Rev. C](#) **41**, 1941 (1990).